

Shallow seismic activity and young thrust faults on the Moon

Thomas R. Watters¹, Renee C. Weber², Geoffrey C. Collins³, Ian J. Howley², Nicholas C. Schmerr⁴ and Catherine L. Johnson^{5,6}

1. Center for Earth and Planetary Studies, Smithsonian Institution, Washington, DC 20560, USA.

2. NASA Marshall Space Flight Center, Huntsville, AL 35805, USA.

3. Physics and Astronomy Department, Wheaton College, Norton, MA 02766, USA.

4. University of Maryland, Department of Geology, College Park, MD 20742, USA.

5. Dept. of Earth, Ocean and Atmospheric Sciences, University of British Columbia, Vancouver, British Columbia, V6T 1Z4, Canada.

6. Planetary Science Institute, Tucson, AZ 85719, USA.

Correspondence and requests for materials should be addressed to ¹T.R. Watters (e-mail: watterst@si.edu).

March 19, 2019

Abstract

The discovery of young thrust faults on the Moon is evidence of recent tectonic activity, but how recent is unknown. Seismometers at four Apollo landing sites recorded 28 shallow moonquakes between 1969 and 1977. Some of these shallow quakes could be associated with activity on the young faults. However, the epicenter locations of these quakes are poorly constrained. Here we present more accurate estimates of the epicenter locations, based on an algorithm for sparse seismic networks. We find that the epicenters of eight near-surface quakes fall within 30 km of a fault scarp, the distance of expected strong ground shaking. Analyzing the timing of these eight events, we find that six occurred when the Moon was less 15,000 km from the apogee distance. Analytical modeling of tidal forces that contribute to current lunar stress state indicates that seven near-apogee events within 60 km of a fault scarp occur at or near the time of peak compressional stresses, when fault slip events are most likely. We conclude that the proximity of moonquakes to the young thrust faults together with evidence of regolith disturbance and boulder movements on and near the fault scarps, strongly suggests the Moon is tectonically active.

Main

The Lunar Reconnaissance Orbiter (LRO) mission has contributed a new chapter in our understanding of the tectonic evolution of the Moon. High resolution 0.5 to 2 m/pixel images obtained by the Lunar Reconnaissance Orbiter Camera (LROC) have revealed a vast, global network of lobate fault scarps^{1,2}. These scarps are interpreted to be the results of thrust faults based on morphology, crosscutting relations, reversals in vergence, segment linkage, and modeling¹⁻⁵. Their small scale and crisp appearance, crosscutting relations with small-diameter impact craters, and buffered and traditional crater size-frequency distribution dating indicate the fault scarps are very young^{1,2,6} (Fig. 1). Expected rates of infilling of associated small, shallow graben suggests

the lobate scarps are <50 Ma old⁷. Such a young age raises the intriguing possibility that these thrust faults are currently active.

The population of young thrust fault scarps provides a window into the recent stress state of the Moon and offers insight into the origin of global lunar stresses (Fig. 2A). The widespread spatial distribution of the thrust fault scarps confirms that the Moon has recently undergone global contraction. However, analysis of the orientations of the fault scarps shows that the distribution of orientations is non-random², inconsistent with isotropic stresses from global contraction. The orientations of the fault scarps are suggestive of the influence of tidal forces, and modeling shows that tidal stresses contribute significantly to the current stress state of the lunar crust². Tidal stresses (orbital recession and diurnal tides) superimposed on stresses from global contraction result in non-isotropic compressional stress consistent with the thrust fault scarp orientations. At any particular point on the lunar surface, peak compressive stress will be reached at a certain time in the diurnal cycle. At apogee, the addition of diurnal and recession stresses are most compressive near the tidal axis, while at perigee they are most compressive 90° away from the tidal axis. Coseismic slip events on currently active thrust faults are most likely triggered when peak stresses are reached².

Lunar seismicity was recorded by four seismometers that were placed at the Apollo 12, 14, 15 and 16 landing sites. These seismometers operated from 1969 to 1977 and recorded 28 shallow moonquakes⁸⁻¹⁰ (Fig. 2A). Analysis of the shallow moonquakes indicated Richter-equivalent magnitudes in the range from 1.5 to ~5 and body wave magnitudes >5.5 with estimated stress drops of ≤10 MPa for 16 events and >10 MPa for 11 events¹⁰⁻¹². Three of these shallow moonquakes are estimated to have stress drops of ≥100 MPa (11, 12). The large stress drops

reported for some of the shallow seismic events may be due to pre-slip accumulated stress on the faults.

The current best epicenter determinations for most shallow moonquake locations are likely only accurate to several degrees (60 – 90 km), and are even less accurate for small and/or more distant events from the seismometers. Shallow moonquake depths are also poorly constrained^{8-10,13,14}, with some estimated to occur at the surface and others up to depths of 200 km. A recent analysis suggests they originate at depths of 50 ± 20 km (14). Although the quality of the Apollo seismic data imposes limits on the accuracy of hypocenter locations, establishing connections between the recorded shallow moonquakes and young tectonic landforms may indicate currently active lunar faults.

Shallow moonquake location and depth uncertainties make a direct comparison with the locations of known tectonic features challenging. Here, we analyze the timing, and reevaluate the epicentral locations and depths of shallow moonquakes recorded by the Apollo Seismic Network to investigate the hypothesis that shallow moonquake seismic events represent activity on young thrust faults. We also examined the relationship between shallow moonquake timing and locations to the stress state of the Moon to determine whether moonquakes occur at the times and locations of predicted peak stresses.

Relocating Shallow Moonquakes

It is first necessary to improve the accuracy of the epicentral locations and depths of shallow moonquakes. Past epicenters were determined using the standard method for locating a seismic event that uses a known velocity model and the observed arrival times of the direct P and S waves^{8-10,14}. The reported large uncertainties in arrival times directly translated into the large uncertainties in these event locations. To refine the locations, we applied a relocation algorithm

(LOCSMITH) specifically adapted for using inaccurate data from very sparse seismic networks^{16,17} requiring only arrival time uncertainties. Rather than solving for a best-fit location, this approach divides the solution set into falsified and non-falsified candidate locations using an adaptive grid search, and accounts for arrival time uncertainty using windows around the true arrival time. The result for each event is not a single location, but a cloud of candidate locations (Supplementary Information) (Fig. 2B). Of the 28 total shallow moonquakes identified by Nakamura et al.⁸⁻¹⁰, 13 have confirmed locations (the location cloud contains the original epicentral location), 7 resulted in binary location clouds (two separate clouds of epicenters that do not contain the original location), and 8 have fragmented location clouds (the relocated epicenters are not well constrained and are widely scattered). Acceptable locations occur at depths up to 300 km, beyond which the search was terminated. However, since modeling of the faults associated with the scarps indicates the depth of faulting is likely no more than 1 km (5, see Supplementary Information) only clouds with surface locations were evaluated. Although surface solutions for the shallow moonquakes have been obtained in previous studies, deeper crustal sources have also been suggested^{8-10,13}, based on scattering properties of the lunar crust observed in the Apollo seismic data¹⁴. However, measurements of the scattering properties show that the decay times of the population of surface impact events have substantial overlap with the shallow moonquake population^{14,15}, supporting near-surface sources for shallow moonquakes (see Supplementary Information).

Of the 20 relocated shallow moonquakes, 13 confirmed and 2 binary point clouds have solutions at the surface for a total of 17 possible epicentral locations (Fig. 2B). All 17 clouds or clusters of relocated epicenters either encompass or are near a mapped scarp (Fig. 2B). Among the 17 clouds and clusters of equally viable locations, 17 epicenters were selected based on their

proximity (minimum distance) to a mapped fault scarp. Distances between the relocated epicenters and mapped fault scarps range from ~3 to 292 km. In order to more confidently associate a given hypocenter to a mapped scarp, a limiting distance beyond which a moonquake and a fault are considered unrelated must be established.

Ground movement from shallow moonquakes occurs over an area dependent on the magnitude of the seismic event. Seismic waves are much less attenuated in the Moon than in the Earth, and intense scattering of seismic waves in the heavily fractured lunar megaregolith diffuses surface and body wave energy into more than 1-hour-long seismic codas^{18, 19}. Evidence for strong seismic shaking in the vicinity of these faults is found in degraded and missing small crater populations extending many kilometers away from the scarps⁶. Additional evidence is found in crater degradation rates. The degradation rate of small craters in basalts of the Apollo 17 Taurus-Littrow valley (~20.1°N, 30.7°E) is higher than in the Apollo 16 Cayley plains (~9°S, 15.5°E), and the depth-diameter ratio of the degraded craters does not change as a function of distance from the Lee-Lincoln scarp (a distance of >15 km)²⁰. This suggests the possibility of strong seismic shaking throughout the entire Taurus-Littrow valley from slip events on the Lee-Lincoln thrust fault.

In an effort to evaluate the distance from a fault scarp where significant ground movement is expected from a shallow moonquake, we modeled the seismic shaking for an event on a typical lobate scarp in the Mandel'shtam cluster (Supplementary Information). The maximum seismic moment is equated to the total seismic moment estimated from the best fitting parameters for the geometry, depth, and cumulative displacement on the fault obtained from elastic dislocation modeling constrained by the topography of the Mandel'shtam scarp (Supplementary Fig. S1, S2). Employing the terrestrial shaking intensity scale based on Worden et al.²¹, the distance from the

Mandel'shtam scarp within which peak shaking is Strong (Supplementary Information) for the vertical ground motion component is ~ 30 km, and for the horizontal component is ~ 17 km (Fig. 4). We thus propose that the effects of seismic shaking from a slip event on a typical scarp can extend to ~ 30 km ($\sim 1^\circ$ on the lunar surface), and we use this estimate to define the limiting distance beyond which a relocated epicenter and a proximal fault scarp are unrelated. If peak shaking at the Moderate level is included, the limiting distance could be extended to ~ 60 km (Fig. 4).

Sources and Timing of Events

Analysis of the minimum distance between the relocated epicenters and the lobate scarps indicates that eight of the 17 epicenters are within our criteria of 30 km (Fig. 2B, Supplementary Fig. S3A). To test if the proximity of the eight relocated epicenters is random, 10,000 sets of 17 random epicentral locations were generated. The results show that $<4\%$ of these 170,000 random quake locations occur within 30 km of a fault scarp (Supplementary Fig. S3B) and that none of the 10,000 sets produce more than five random quake locations within 30 km of a scarp (Supplementary Fig. S3C). Even doubling the minimum distance, only three of the 10,000 sets have 8 or more random quake locations within 60 km of a scarp (Supplementary Fig. S3D). This suggests that the close proximity of many of the relocated epicenters to mapped scarps is not random.

We next related the recorded origin times for the shallow moonquakes to the Earth-Moon distance (EMD) over the course of the Apollo seismic experiment. This revealed that of the 28 shallow moonquakes, 18 occur when the Moon is closer to apogee (Fig. 3A), while 8 events occur closer to perigee and 2 occur between apogee and perigee. In the EMD plot (Fig. 3A), a longer 206-day modulation due to the Sun's perturbations on the lunar orbit is visible in addition to the monthly variation. Demodulating the time series (Supplementary Fig. S4) shows an evident

non-random distribution in the timing of the shallow moonquakes (Fig. 3B). The 18 shallow moonquakes that occur near apogee are within 15,000 km of the apogee distance at the time of the events (Fig. 3C). This grouping of events may reflect that the Moon orbital velocity is almost 114 m/s slower at apogee than at perigee, so there is more time for stresses that accumulate near and at apogee than any other place in the Moon's orbit. Thus, we define events that occurred within 15,000 km of the apogee distance to be “near apogee” events. We tested the possibility that the observed grouping of a small number of shallow moonquakes recorded by the Apollo Seismic Network near apogee and perigee is a random effect by generating 10,000 sets of 28 random events. By comparison with the recorded events, the median number of events in the 10,000 random sets within 15,000 km of apogee is 12; less than 4% of the random sets have 18 or more quakes within 15,000 km of apogee (Fig. 3D). Moreover, the distribution of random quakes is approximated by a normal distribution (Fig. 3D). The probability p of a random set having 18 out of 28 quakes occurring within 15,000 km of apogee is ~ 0.01 . We conclude the observed grouping of events that occurred near apogee is not simply an artifact of the small sample size. Thus, of the eight relocated epicenters with surface solution within 30 km a fault scarp, six are in the set of 18 moonquakes that occur within 15,000 km of apogee (Supplementary Table S3). If the limiting distance is extended to ~ 60 km, two additional moonquakes occur within 15,000 km of apogee (Supplementary Table S3).

If the shallow moonquakes that occur at apogee are related to coseismic slip events on the thrust fault scarps, their epicentral locations should correspond to regions of peak near-surface stress. The current stress state of the Moon is dominated by radial contraction from interior cooling, contributing an estimated ≥ 2 but < 10 MPa based on the currently mapped population of lobate thrust fault scarps^{1,2}. Superimposed on compressional stresses from contraction σ_c are two

components of tidal stress, orbital recession stress σ_r and diurnal stress σ_t . Modeling the tidal stresses^{22,23} shows they are dominated by σ_r that may reach >200 kPa (Supplementary Information). An additional component of stress that may contribute to the current lunar stress state is polar wander (see 23). True polar wander has been attributed to a change in the Moon's moments of inertia due to a low-density thermal anomaly beneath Procellarum²⁴. The change in the location of the poles is consistent with the observed remnant polar hydrogen deposits²⁴. Stresses from $\sim 3^\circ$ of polar wander σ_w over the last 1 billion years are on the order of ± 8 kPa (see Supplementary Information) (Fig. 5).

Modeling shows that the maximum compressional stresses occur at apogee when stresses peak at a minimum of more than 2.2 MPa near sub-Earth and anti-Earth points. Model strength envelopes for the lunar near-surface indicate stresses of $\sim 2\text{--}7$ MPa are sufficient for shallow thrust faults to develop⁵. Peak compressional stresses >2 MPa extend well beyond the regions around the tidal axes, encompassing much of the lunar surface (Fig. 5). Due to the libration of the sub-Earth point, the local maximum compressional stress at any particular location on the lunar surface may occur a few days before or after apogee. An examination of the six near-apogee, relocated shallow moonquakes within 30 km of a fault scarp shows that all are located in regions where the peak stress is >2 MPa. A further analysis of stress levels around the times and locations of the six near-apogee shallow moonquakes indicates that five occur at or near peak compression, or closely before or after peak compressional stresses are reached (Fig. 5) (Supplementary Fig. S6, Table S3). Extending the limiting distance to 60 km permits two other events to meet this condition (Fig. 5, Supplementary Table S3).

Evidence of Recent Activity

Lobate scarps in proximity to relocated moonquakes with surface solutions are prime candidates for recent activity and thus identifiable surface expressions. Evidence of activity may be expressed by disturbed regolith from downslope creep or landslides that expose fresh material with a higher albedo than the surrounding mature regolith darkened by space weathering. Boulder fields that occur in relatively high albedo patches may also be evidence of recent surface change. Such features might be expected on the relatively steeply sloping scarp face or on nearby higher sloping surfaces such as impact crater walls. Examples of fresh boulder fields are found on the slopes of a scarp in the Vitello cluster (Fig. 6A) and examples of possible albedo features are associated with scarps that occur near craters Gemma Frisius C and Mouchez L (Fig. 6B, C). These albedo features are on the scarp faces and at the bases of the scarps and cannot be accounted for as simple lighting or viewing geometry artifacts.

Another line of evidence for recent activity are boulder movements or falls expressed by tracks made as the boulder rolls and bounces downslope. Boulders are commonly found along or near scarp faces¹ and may have accumulated by downslope movement triggered by coseismic slip events on the related thrust faults. Boulder tracks near lobate scarps in Schrödinger basin were attributed to recent boulder falls induced by seismic shaking²⁵.

The Lee-Lincoln scarp is ~13 km from a relocated epicenter in the Taurus-Littrow valley, which hosts the Apollo 17 landing site (Fig. 2B). Boulders and boulder tracks on the slopes of North Massif were examined by the Apollo 17 astronauts²⁶. Boulders located at the Apollo 17 Stations 6 and 7 are ~5 km from the Lee-Lincoln scarp (Fig. 6D). In addition to boulder falls and the degraded small craters in the Taurus-Littrow valley, a large landslide on South Massif that covered the southern segment of the Lee-Lincoln scarp and debris flows in the Sculptured Hills may be further evidence of possible coseismic slip events^{27, 28}.

Evidence of seismic shaking may also be expressed by boulders on the interior slopes of a small, degraded crater located near a scarp face that are aligned in rows paralleling the orientation of the scarp (Fig. 6E). As described previously, seismic shaking can result in under-represented or missing size ranges and effect the degradation rate of small impact craters^{6,20}.

A search for evidence of very recent change (during the LRO mission) using temporal pairs of LROC NAC images may provide the best case for current activity on the population of young thrust faults. The ultimate test of our hypothesis that shallow seismic events are related to the young thrust faults and that the occurrence of coseismic slip events is greater when the Moon is near or at apogee would be achieved by the deployment of a new long-lived Lunar Geophysical Network. In particular, such a network could investigate the distribution of farside shallow quakes and events on other nearside faults.

Methods

Details about the methods used in this paper can be found in the Supplementary Information.

Data Availability

The images and data used in this study are available on the Smithsonian's National Air and Space Museum Data Repository website (<https://airandspace.si.edu/research/data-repository>).

The raw and calibrated image data that support the findings of this study are available from Planetary Data System Cartography and Imaging Sciences Node, LROC Data Archive at the LROC Data Node http://wms.lroc.asu.edu/lroc/rdr_product_select.

References

1. Watters, T. R. *et al.* Evidence of recent thrust faulting on the Moon revealed by the Lunar Reconnaissance Orbiter Camera. *Science*, **329**, 936-940 (2010).

2. Watters, T. R. *et al.* Global thrust faulting on the Moon and the influence of tidal stresses. *Geology*, **43**, 851–854 (2015).
3. Watters, T. R. & Johnson, C. L. Lunar Tectonics. *In Planetary Tectonics*, T. R. Watters, R. A. Schultz, Eds. (Cambridge Univ. Press, New York, NY, 2010), pp. 121–182.
4. Banks, M. E. *et al.* Morphological analysis of lobate scarps on the Moon using data from the Lunar Reconnaissance Orbiter. *J. Geophys. Res.*, **117**, doi :10.1029/2011JE003907 (2012).
5. Williams, N. R. *et al.* Fault Dislocation Modeled Structure of Lobate Scarps from Lunar Reconnaissance Orbiter Camera Digital Terrain Models. *J. Geophys. Res.*, doi: 10.1002/jgre.20051 (2013).
6. van der Bogert, C. H. *et al.* How old are lunar lobate scarps? 1. Seismic resetting of the crater size-frequency distribution. *Icarus*, **306**, 225-242, 2018.
7. Watters, T. R. *et al.* Recent extensional tectonics on the Moon revealed by the Lunar Reconnaissance Orbiter Camera. *Nature Geoscience*, **5**, doi:10.1038/NGEO1387, 181 (2012).
8. Nakamura, Y. *et al.* Shallow moonquakes: Depth, distribution and implications as to the present state of the lunar interior. *Proc. Lunar Sci. Conf. 10th*, 2299-2309 (1979).
9. Nakamura, Y. *et al. Tech. Rep. 118*, Inst. for Geophys., Univ. of Tex. Austin (1981).
10. Nakamura, Y., Latham, G.V., & Dorman, H. J. Apollo lunar seismic experiment – Final summary. *J. Geophys. Res.*, **87**, A117-A123 (1982).
11. Oberst, J. Unusually high stress drops associated with shallow moonquakes. *J. Geophys. Res.*, **92(B2)**, 1397–1405, doi:10.1029/JB092iB02p01397 (1987).
12. Binder, A. B., & Oberst, J. High stress shallow moonquakes: evidence for an initially totally molten Moon. *Earth, Planet. Sci. Letts.*, **74**, 149-154 (1985).
13. Lognonné, P., Gagnepain-Beyneix, J. & Chenet, H. A new seismic model of the Moon: implication in terms of structure, thermal evolution and formation of the Moon. *Earth Plan. Sci. Let.*, **211**, 27-44 (2003).
14. Gillet, K., Magerin, L. Calvet, M. & Monnereau, M. Scattering attenuation profile of the Moon: Implications for shallow moonquakes and the structure of the megaregolith. *Phys. Earth and Planet. Inter.*, **262**, 28-40 (2017).
15. Blanchette-Guertin, J. -F., Johnson C. L. & Lawrence, J. F. Investigation of scattering in lunar seismic coda. *J. Geophys. Res.*, **117**, E06003, doi:10.1029/2011JE004042 (2012).

16. Knapmeyer, M. Location of seismic events using inaccurate data from very sparse networks. *Geophys. J. Int.*, **175**, 975-991, (2008).
17. Weber, R. C., Knapmeyer, M., Panning, M. & Schmerr, N. Modeling approaches in planetary seismology, in *Extraterrestrial Seismology*, V. C. H. Tong, R. A. Garcia, Eds. (Cambridge Univ. Press, New York, NY, 2015), pp. 140–158.
18. Nakamura, Y & Koyama, J. Seismic Q of the lunar upper mantle. *J. Geophys. Res.*, **87**, 4855-4861 (1982).
19. Oberst, J. & Nakamura, Y. A seismic risk for the lunar base. The Second Conference on Lunar Bases and Space Activities of the 21st Century (NASA), Vol. 1, 231-233 (1985).
20. Mahanti P., Robinson, M. S., Thompson, T. J. & Henriksen, M. R. Small lunar craters at the Apollo 16 and 17 landing sites – morphology and degradation. *Icarus*, **299**, 475-501 (2018).
21. Worden, C. B., Gerstenberger, M. C., Rhoades, D. A. & Wald, D. J. Probabilistic relationships between ground-motion parameters and modified Mercalli intensity in California. *Bull. Seism. Soc. Am.*, **102**, 204-221 (2012).
22. Matsuyama, I. & Nimmo, F. Tectonic patterns on reoriented and despun planetary bodies. *Icarus*, **195**, 459-473 (2008).
23. Collins, G. C., *et al.* Tectonics of the outer planet satellites. in *Planetary Tectonics*, T. R. Watters, R. A. Schultz, Eds. (Cambridge Univ. Press, New York, NY, 2010), pp. 264–350.
24. Siegler, M. A. *et al.* Lunar true polar wander inferred from polar hydrogen. *Nature*, **531**, 480-484 (2016).
25. Kumar, P. S. *et al.* Recent shallow moonquake and impact-triggered boulder falls on the Moon: New insights from the Schrodinger basin. *J. Geophys. Res.*, **121**, 147–179 (2016).
26. Arvidson, R., Drozd, R. J., Hohenberg, C.M., Morgan C. J. & Poupeau, G. Horizontal transport of the regolith, modification of features, and erosion rates on the lunar surface. *The Moon*, **13**, 67-79 (1975).
27. Schmitt H. H. *et al.* Revisiting the field geology of Taurus-Littrow. *Icarus*, **298**, 2-33 (2017).
28. van der Bogert, C. H. *et al.* Derivation of absolute model ages for lunar lobate scarps, *LPSC 43*, Abstract #1847 (2012).

Acknowledgements

We thank Amanda Nahm and Taichi Kawamura for their thoughtful comments and suggestions that greatly improved the manuscript, and we also thank M.S. Robinson and the LROC team.

We gratefully acknowledge the LRO engineers and technical support personnel. This work (TRW) was supported by the LRO Project and an ASU LROC Contract. CLJ acknowledges support from the Natural Sciences and Engineering Research Council of Canada.

Author contributions

T.R.W. drafted the manuscript. R.C.W. and I.J.H. relocated the shallow moonquakes and R.C.W. analyzed timing and Earth-Moon distance, G.C.C. modeled stress magnitudes and orientations, N.C.S. generated the seismic shake maps, and C.L.J. and R.C.W. assisted with the statistical analysis. All of the authors contributed to the interpretation and analysis.

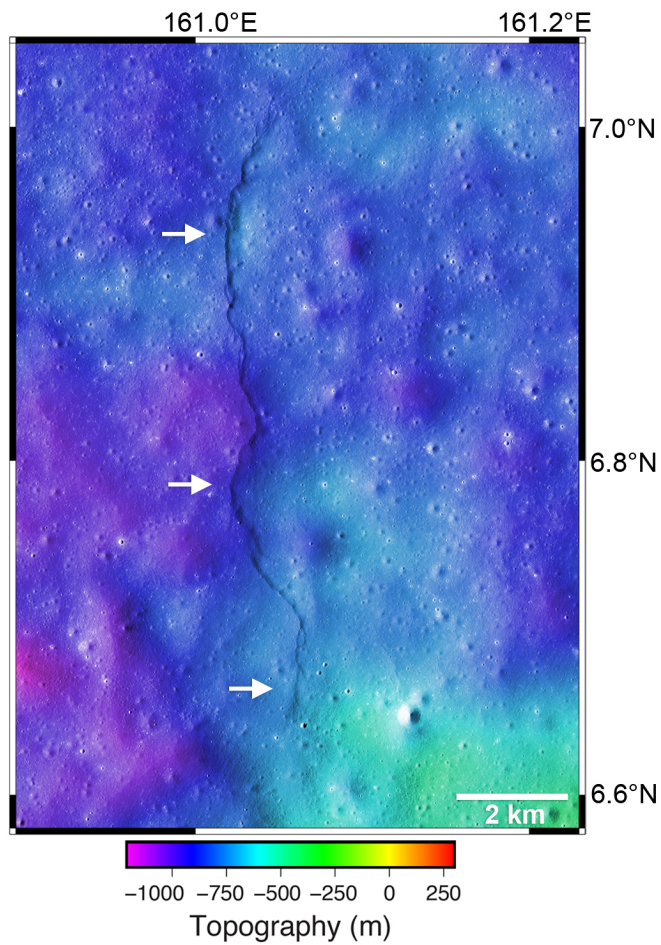


Figure 1. A prominent lobate thrust fault scarp in the Mandel'shtam Cluster located in the farside highlands (6.9°N, 161°E) is one of thousands discovered in LROC images. Digital elevation model of the Mandel'shtam scarp was generated using LROC NAC stereo images (frames M191895630 and M191909925). The scarp (white arrows) has a maximum relief of ~70 m. The DEM has a horizontal spatial scale of 5 m/pixel (NAC stereo images have a resolution of ~1 m/pixel) and a vertical precision of ~0.5 m. Elevations are referenced to a sphere of 1,737,400 m.

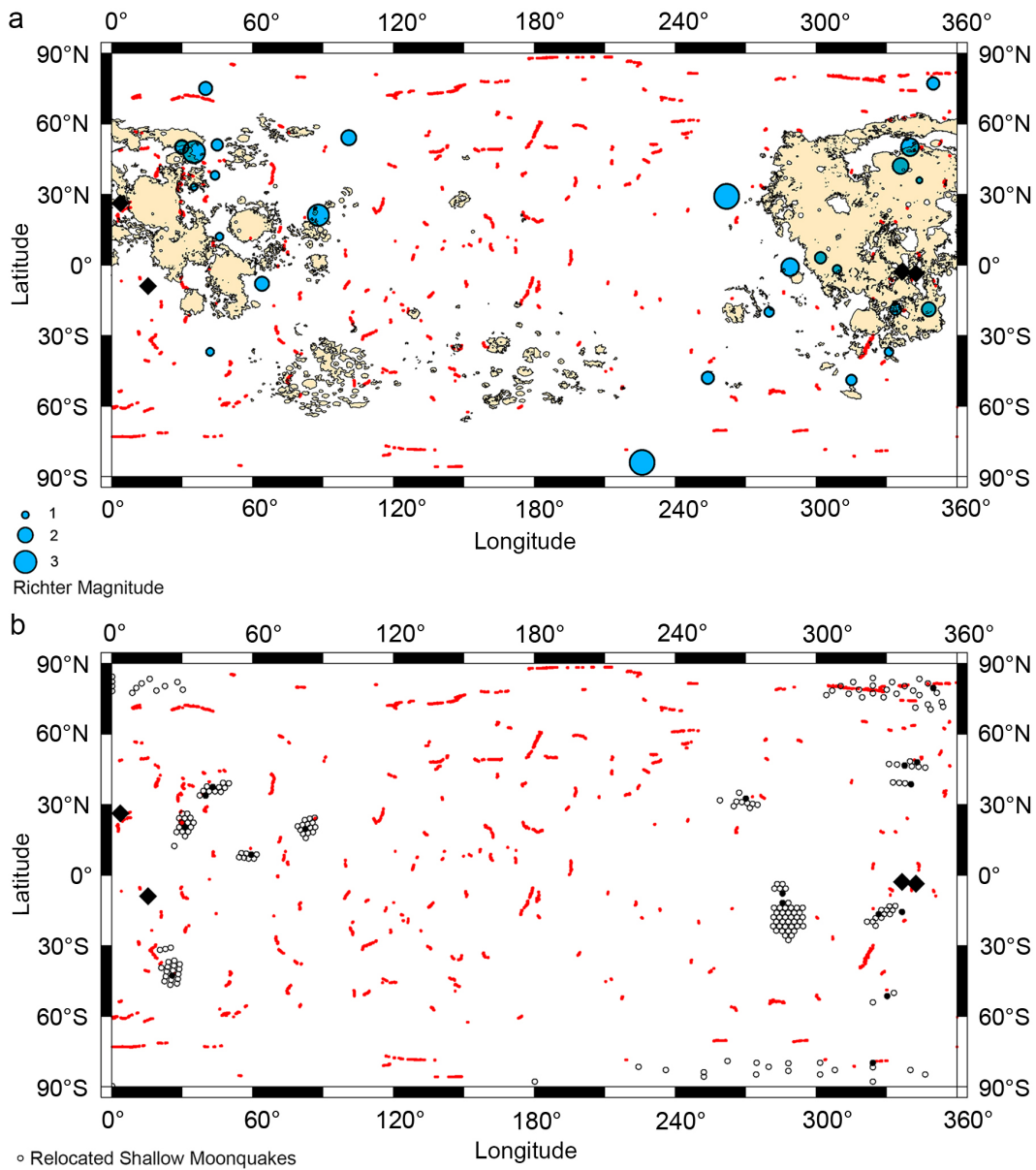


Figure 2. Maps showing the locations of young lobate thrust fault scarps and shallow moonquakes. (a) Map shows locations of 3,543 lobate scarps^{1,2} (red), published epicentral locations of shallow moonquakes (blue dots)⁹, and locations of Apollo Seismic Network seismometers (black diamonds). Moonquake symbol size is scaled by estimated Richter magnitude¹⁰. Mare basalt units are shown in tan. (b) Relocated epicenter clouds of shallow moonquakes with solutions at the surface. Locations of 17 possible epicenters (blue circles) in

the relocated clouds and clusters are indicated (black circles). Mapped lobate scarps (red) and Apollo Seismic Network seismometer locations (black diamonds) are show in (a) and (b).

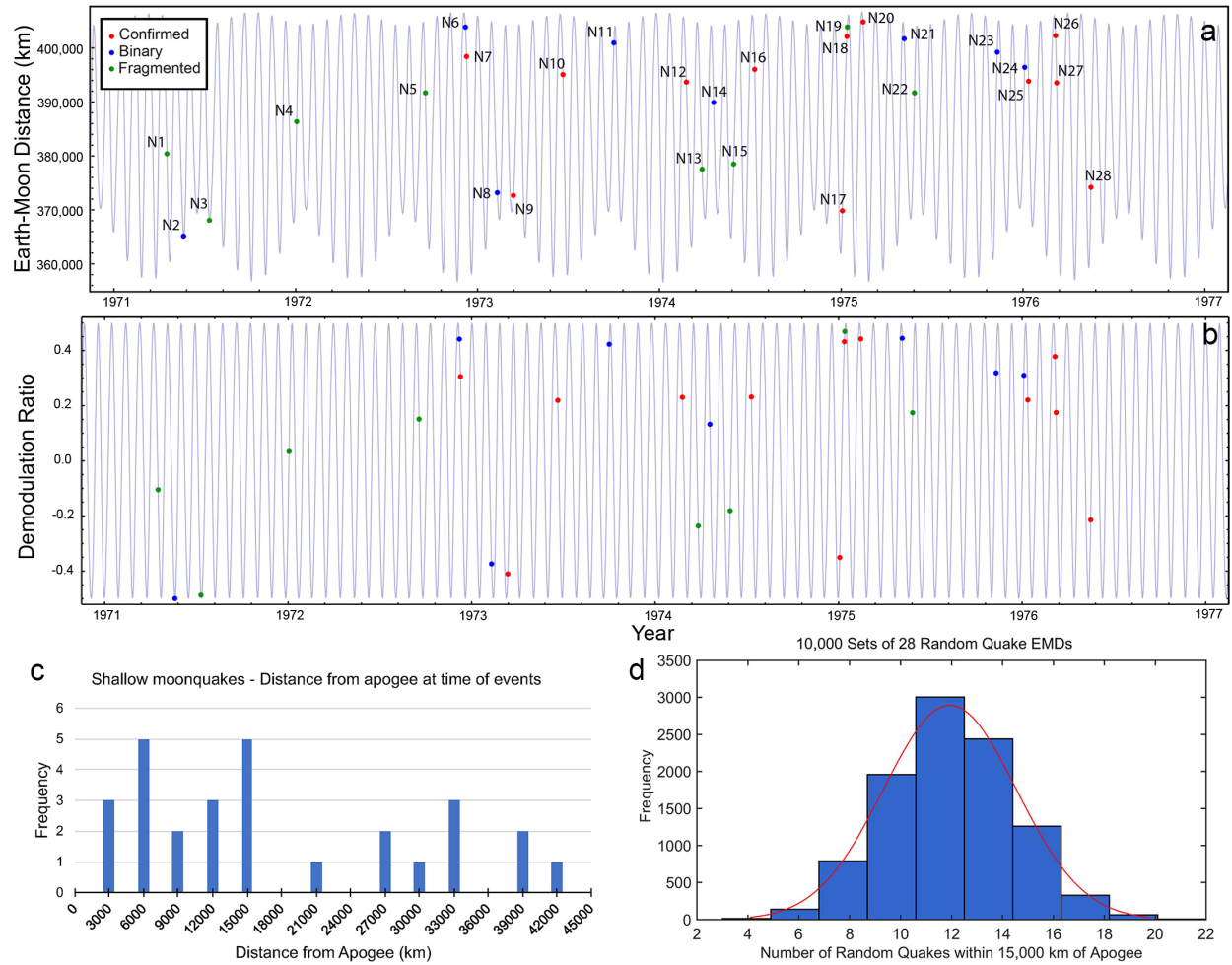


Figure 3. Earth-Moon distance (EMD) over the course of the Apollo seismic experiment. (a) Shallow moonquakes are indicated by dots, color indicates classification of the epicenter relocation clouds (red, confirmed; blue, binary; green, fragmented). In addition to the monthly variation, a longer on the lunar orbit can be seen. (b) Demodulated plot removes the 206-day modulation due to the Sun's perturbations leaving only the monthly variation. Of the 18 events close to apogee, 6 are approaching apogee and 12 are departing. (c) Histogram of the EMD from apogee at shallow moonquake times. Eighteen of the 28 shallow moonquakes occur when the

Moon is less than 15,000 km of apogee, defined as “near apogee” events. (d) Histogram of number of events in 10,000 random sets of 28 quakes within 15,000 km of apogee. The random quake events were generated from a timing distribution that is uniform between the first and last recorded shallow moonquake. The number of random quakes within 15,000 km of apogee is well approximated by a normal distribution (red line).

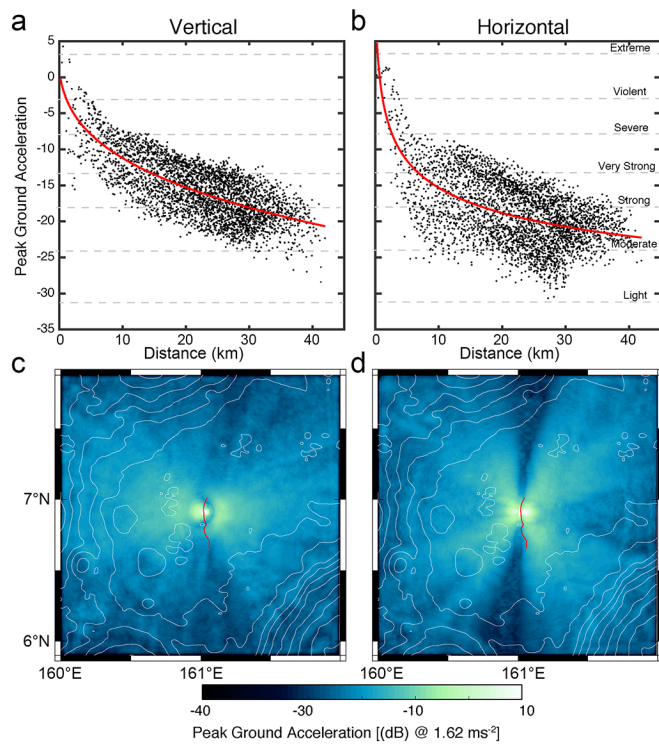


Figure 4. Seismic shakemaps and expected ground motion for a slip event on a thrust fault in the Mandel'shtam cluster. Plots show the decay in vertical (a) and horizontal (c) shaking from the epicenter. Shakemaps show peak vertical (b) and horizontal (d) acceleration for a 6.36 M_w hypocenter at 6.91°N and 161.02°E and 350 m depth (Supplementary Information). For (b) and (d) the Mandel'shtam thrust fault is shown by the red lines and regional topography is shown by the white contour lines (500 m contour interval). Acceleration is given in decibels, where $1 \text{ dB} = 20 \log_{10} (A/A_{ref})$ where A is the amplitude and A_{ref} is the reference lunar gravity (1.62 m/s^2), so a

40 dB difference between locations is ~ 100 times lower amplitude. Red lines are the best fitting power laws to the distributions of points in the vertical and horizontal components of motion (r^2 of 0.54 and 0.33 respectively).

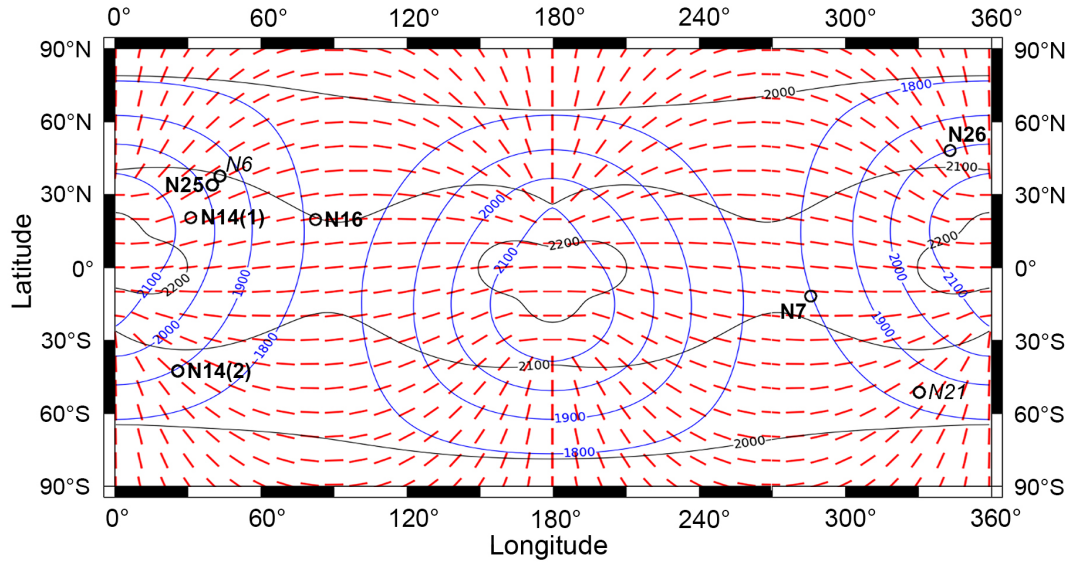


Figure 5. Current near-surface stress state of the Moon. Modeled stresses are: 1) 2 MPa of isotropic compression from global contraction, 2) orbital recession, 3) 3° of true polar wander (TPW), and 4) diurnal tidal stress at apogee. Contours of most and least compressive stress magnitudes shown by black and blue lines, respectively (100 kPa contour interval). Orientations of the maximum compressive stress are shown by red lines. Relocated shallow moonquakes within 30 km of a fault scarp that occur near apogee are shown by black circles (bold N#) along with moonquakes within 60 km of a scarp (italic N#) (see Fig. 3A, Table S3).

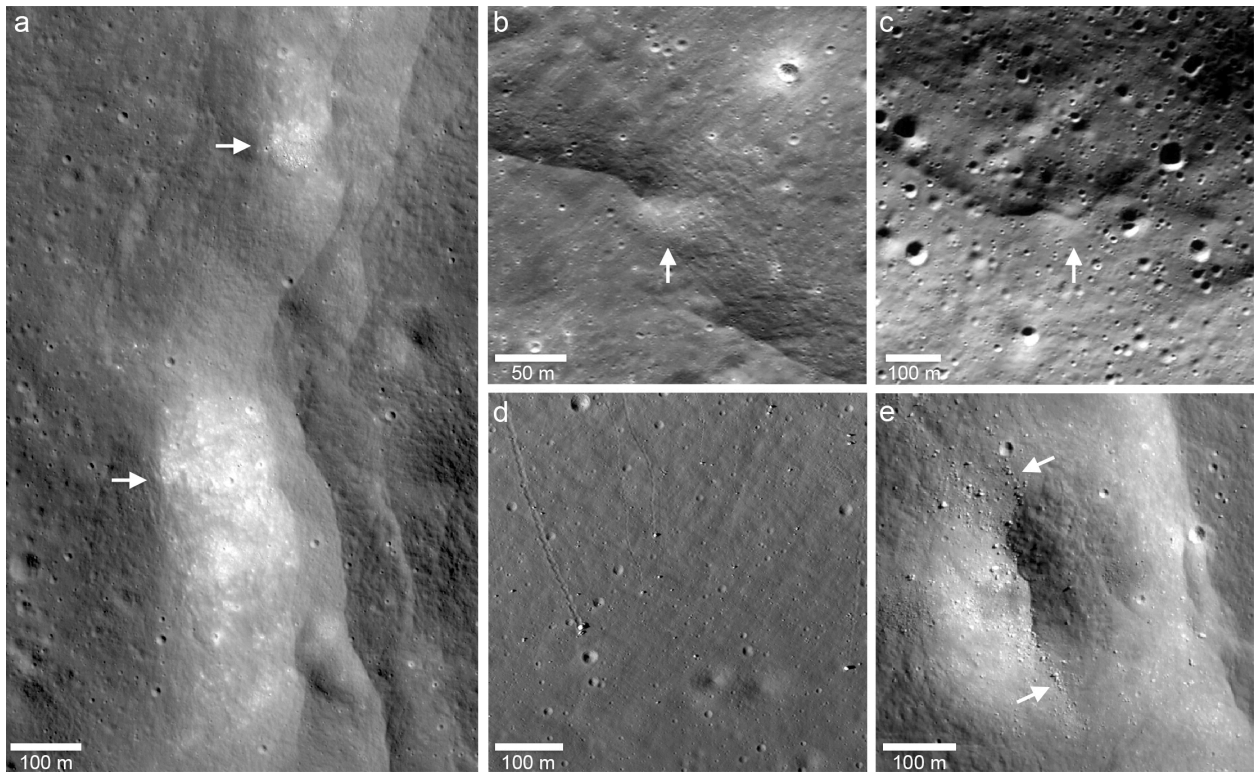


Figure 6. Possible evidence of recent activity on fault scarps near relocated shallow moonquakes.

(a) A prominent lobate scarp in the Vitello Cluster (34.4°S , 37.9°W). Boulder fields characterized by patches of relatively high albedo regolith occur on the scarp face and back scarp terrain (white arrows). Image LROC NAC frame M190844037LR. (b) Albedo feature on the scarp face of the Gemma Firsuis C lobate scarp (white arrow) (36.1°S , 18.7°E). The scarp is ~ 120 km from the closest relocated epicenter. NAC image frame M124449632R. (c) Albedo feature on the scarp face of the Mouchez L lobate scarp (white arrow) (77.9°N , 36.3°W), ~ 25 km from the closest relocated epicenter. NAC image frame M1119172889L. (d) Boulders and boulder tracks on the slopes of North Massif (20.3°N , 30.8°E), ~ 5 km east of the Lee-Lincoln scarp. The large boulder is the Apollo 17 Station 6 boulder. The scarp is ~ 11 km from the closest relocated epicenter in the Taurus-Littrow valley. NAC image frame M134991788R. (e) Boulders in an ~ 300 m diameter degraded crater in the back scarp terrain of the Vitello lobate scarp have

aligned in rows that parallel the orientation of the fault scarp (34.69°S , 37.89°W). NAC image frame M190844037L.